

Measuring effect of the blooming of chemical curatives on the rate of cyclic fatigue crack growth in natural rubber filled with a silanized silica nanofiller

Farhan Saeed¹, Ali Ansarifar^{1*}, Robert J Ellis², Yared Haile-Meskel²

Department of Materials, Loughborough University, Leicestershire LE11 3TU, UK

ABSTRACT

Two rubber compounds with different amounts of chemical curatives were prepared by mixing natural rubber with a high loading of a sulfur-bearing silanized precipitated amorphous white silica nanofiller. The chemical bonding between the filler and rubber was optimized via the tetrasulfane groups of the silane by adding a sulfenamide accelerator and zinc oxide. The rubber compounds were cured and stored at ambient temperature for 65 days before they were tested. One compound showed extensive blooming as a function of storage time. Thin tensile strips of the rubber vulcanizates containing an edge crack were repeatedly stressed at constant strain amplitude and test frequency at ambient temperature and crack length c was measured as a function of the number of cycles n . The cut growth per cycle, dc/dn , was calculated and plotted against the tearing energy, T . The blooming of the chemical curatives increased dc/dn by up to an order of magnitude at a constant T . This was due to the

* Correspondence to: A. Ansarifar (M.A.Ansarifar@lboro.ac.uk).

² DTR VMS Ltd, Bumpers Way, Chippenham, Wiltshire SN14 6NF, United Kingdom.

re-agglomeration of the chemical curatives in the rubber and also within a thin layer

approximately 15-20 μm in size beneath the rubber surface. Under repeated stressing, cracks

grew through the relatively weak agglomerated areas in the rubber and this caused the rate of

crack growth to increase at a constant T.

Key words: rubber, additives, silicas, blooming, fatigue analysis

INTRODUCTION

Elastomers or rubbers are probably one of the most versatile groups of polymers ever known

to man. Rubbers are elastic over a wide range of applied stresses and are used to manufacture

articles such as engine mountings, isolation bearings, tires and belts for dynamic service

applications. In most applications of rubber, the functioning, durability and service life of the

component depends on the properties of the rubber and when fatigue or other types of failure

occur the device ceases to function properly or fails altogether. "Fatigue is used in the sense

of a progressive "action" or failure, resulting in unserviceability of the rubber article, during

use."¹ There are various factors involved in fatigue of rubber, e.g. inhomogeneities, voids

and re-agglomeration of materials normally dispersed in rubber during mixing.

Inhomogeneities are particles of pigment, foreign material and areas of unequal cure, and serve as loci of fatigue failure by the mechanism of forming highly localized stress concentration.^{2,3}

Industrial rubber articles such as the ones aforementioned, contain chemical ingredients for instance curing agents, accelerators, activators, processing aids, antidegradants and fillers. These chemicals are added during various stages of mixing with the specific aim of dispersing them uniformly throughout the rubber in order to achieve the best possible effect on the downstream processing of the compound and mechanical properties of the cured product. When the solubility of the compounding ingredients in the rubber is low, blooming may occur on the surface. Blooming is a process of diffusion of chemical additives dissolved in the rubber, to the surface, followed by crystallisation. Crystallisation from supersaturated solution takes place more readily on the surface than in the rubber itself. This can be due to lack of equilibrium in concentration, which leads to transport of the ingredients to the surface.⁴

To vulcanize rubber to produce a homogenous product, the chemical curatives must disperse well and remain in the rubber. This can be achieved when the chemicals have a high solubility as well as a high rate of diffusion in the rubber.⁴ Studies have shown that accelerators, e.g. sulfenamide types, diffuse to the surface because they are partly soluble in most rubbers.⁵ This diffusion can be detrimental to rubber properties such as loss of adhesion,^{6,7} and also to the durability and performance of rubber in service as well as to health, safety and the environment.

The aim of this study was to measure effect of the migration of a sulfenamide accelerator to the surface on the hardness and rate of fatigue crack growth of natural rubber filled with a high loading of a silanized silica nanofiller. These properties were measured after the rubber vulcanizate was stored at ambient temperature for 65 days to allow full blooming to appear on the rubber surface.

EXPERIMENTAL

Materials and mixing

The raw elastomer used was standard Malaysian natural rubber grade L (SMRL). The

reinforcing filler was Coupsil 8113, which was supplied by Evonik Industries AG of Germany. Coupsil 8113 is a precipitated amorphous white silica-type Ultrasil VN3 surfaces of which had been pre-treated with bis(3-triethoxysilylpropyl)-tetrasulfide (TESPT), known also as Si69 coupling agent, to chemically bond silica to rubber. It has 11.3% by weight silane, 2.5% by weight sulfur (included in TESPT), a 175 m²/g surface area (measured by N₂ adsorption) and a 20-54 nm particle size.

In addition to the raw rubber and filler, the other ingredients were *N*-tert-butyl-2-benzothiazole sulfenamide (a safe-processing delayed action accelerator with a melting point of 109°C) (Santocure TBBS, Flexsys, Dallas), zinc oxide (ZnO; an activator, Harcros Durham Chemicals, Durham, UK), *N*-(1,3-dimethylbutyl)-*N'*-phenyl-*p*-phenylenediamine (an antidegradant with a melting point of 45°C, Santoflex 13, Brussels, Belgium). The melting temperatures of ZnO and silanized silica were above 1000°C. The cure system consisted of TBBS and ZnO, which were added to fully crosslink the rubber via the sulfur in TESPT (Scheme 1). The antidegradant was added to protect the rubber against environmental ageing by ozone and oxygen.

The compounds were prepared in a Haake Rheocord 90 (Berlin, Germany), a small size laboratory mixer with counter rotating rotors. In these experiments, the Banbury rotors and the mixing chamber were initially set at 48°C and the rotor speed was set at 45 r.p.m. The volume of the mixing chamber was 78 cm³ and it was 58% full during mixing. Polylab Monitor 4.17 software was used for controlling the mixing condition and storing data.

For preparing the rubber compounds, a total mixing time of 16 min was used, which was long enough to fully disperse the silica particles in the rubber. The filler and rubber were placed in the mixing chamber and mixed for 13 min and then TBBS, ZnO and antidegradant were added and mixed for an extra 3 min. In total, two rubber compounds were made (Table I). The procedures for measuring the right amounts of TBBS and ZnO for curing the rubber compounds were described previously.⁸

Finally, when mixing ended, the rubber was recovered from the mixer and milled to a thickness of about 6 mm for further work. The compounds were kept at ambient temperature (21±2°C) for at least 24 h before their viscosity and cure properties were measured.

Viscosity and cure properties of the rubber compounds

The viscosity of the rubber compounds was measured at 100°C in a single-speed rotational Mooney viscometer (Wallace Instruments, Surrey, UK) according to a British Standard.⁹

The results were expressed in Mooney Units (MU).

The scorch time, t_{s2} , which is the time for the onset of cure, and the optimum cure time, t_{95} , which is the time for the completion of cure, were determined from the cure traces generated at $140 \pm 2^\circ\text{C}$ by an oscillating disc rheometer curemeter (ODR) (Monsanto, Swindon, UK).¹⁰ The cure rate index, which is a measure of the rate of cure in the rubber, was calculated using the method described previously.¹¹ The rheometer tests ran for up to 2 h. Figure 1 shows the cure traces produced for the two rubber compounds (Table I). Δ torque, which is the difference between the maximum and minimum torque values on the cure trace of the rubber and indicates crosslink density changes¹² was calculated from these traces.

Test pieces and test procedure

After these measurements were completed, the rubber compounds were cured in a compression mould at 140°C with a pressure of 11 MPa to produce sheets 23 cm by 23 cm in

dimensions by approximately 2.8 mm thick. The sheets were then stored at $21\pm 2^{\circ}\text{C}$ for 65 days before they were used. This time was sufficient to allow full blooming to appear on the rubber surfaces.

Examination of the unstrained rubber surfaces and fracture surfaces after the cyclic fatigue tests

In order to study effect of blooming of the rubber curatives on the rubber surfaces and inspect the internal structure of the test pieces before and after cycling, a Carl Zeiss Leo 1530VP field emission gun scanning electron microscope (FEGSEM) (Carl Zeiss NTS GmbH, Oberkochen, Germany) was used. The composition of solid particles in the rubber was determined by an energy dispersive X-ray (EDX) microanalyser (Phoenix System, EDAX, USA). After the test pieces were cycled and increases in crack length as a function of the number of cycles were measured, the fracture surfaces were examined in the SEM. To study effect of the blooming of chemical curatives on the rubber surfaces, samples 4 mm by 6 mm were cut from the unstrained vulcanized sheets of rubber and examined in the SEM. SEM

photographs were subsequently used to analyse the results.

Analysis of the rubber surfaces by Fourier Transform Infrared Spectrometer

A Fourier transform infrared spectrometer (FTIR-8400S) (Shimadzu Scientific Instruments, USA) (FTIR) was used to provide molecular finger print information in order to positively identify compounding chemical components which underwent surface migration. The migrated layer was gently removed from the rubber surface with a clean blade, mixed and grinded with KBr powder. The mixture was poured into a chamber and pressed manually to form a semi transparent disc 1 mm thick and 10 mm in diameter. The disc was then placed in a sample holder and tested. A similar procedure was used to analyse TBBS, ZnO, antidegradant and silanized silica nanofiller, which were the compounding ingredients. The test produced spectra which were examined to determine the chemical components which underwent surface migration. The chemical composition of the bloom was subsequently identified.

Hardness of the rubber vulcanizates

For determining the hardness of the rubber, cylindrical samples 12.5 mm thick and 28 mm in

diameter, were cured. The samples were stored at $21\pm 2^{\circ}\text{C}$ for up to 65 days and then placed in a Shore A Durometer hardness tester (The Shore Instrument and MFG, New York) and the hardness of the rubber was determined at 20°C after 15-s interval. This was repeated at three different positions on each sample and the median of the three readings was subsequently indicated.¹³

Measurement of the cut growth per cycle of the rubber vulcanizates

Crack growth measurements were carried out on thin tensile test pieces of the vulcanized rubber the length of which was approximately six times the width (152 mm by 25 mm). A small crack about 1 mm in length was inserted in one edge of each test piece as perpendicular as possible to both the major and minor surfaces using a sharp razor blade (Fig. 2). The test piece was then deformed in simple extension by repeated cycling to a constant maximum strain amplitude at a test frequency of 1.4 Hz and being relaxed to zero strain on each cycle. After a conditioning period of a few hundred cycles during which the tip, initially a smooth razor cut, became rough, the crack length c was measured. Crack length c was monitored in situ using a travelling microscope as a function of the number of cycles n . The test piece was

slightly strained before crack length was measured to observe the crack tip and determine the crack length as accurately as possible. From these measurements, c was plotted against n and then the cut growth per cycle dc/dn was read off from the slope of the plot (Fig. 3). This was repeated at different n values on the plot. The dc/dn numbers were subsequently plotted against tearing energy T ¹⁴. For a through thickness edge crack (Fig. 2), the energy release rate in simple extension is given by¹⁵

$$T = 2KWc \quad (1)$$

where W is the strain energy per unit volume in the bulk of the material and K being given by

$$K = \frac{\pi}{\sqrt{\lambda}} \quad (2)$$

where λ is the extension ratio.¹⁶ T is proportional to c , so a single test piece covers a range

of T values. The strain energy density was calculated as a function of the applied strain by

numerical integration of the stress-strain curve and was used to calculate T from the

measured values of cut length and strain and the known value of K .¹⁶ Crack growth rate is

referred to the tearing energy at the maximum strain of the cycle. Note that in determining W

allowance was made for the effect of stress relaxation and set occurring in the rubber during

the course of cut growth. The strain amplitude on the test pieces during the crack growth

measurements reached 40%.

Determination of the strain energy density in the rubber at different strain amplitudes

To calculate the strain energy density at different strain amplitudes at which the crack growth measurements were performed, tensile test pieces 152 mm by 25 mm were stamped out of the cured sheets of rubber ~2.8 mm thick, which were kept in storage at ambient temperature for 65 days before use. The test pieces were repeatedly cycled at a crosshead speed of 60 mm/min at 20°C until the force-extension curve settled to a virtually steady state after 7-10 cycles. Values of the strain energy density, W , were calculated from the area under the retraction curve produced after 1 and 10 cycles as shown in Figure 4 and Figure 5, respectively. Lloyd Nexygen 4.5.1. software was used for storing and processing the load versus deflection data which were subsequently changed into stress-strain data for calculating W .

RESULTS AND DISCUSSION

After compound 1, which had 6 phr TBBS and 0.3 phr ZnO chemical curatives (Table I), was mixed, it was subsequently cured to produce thin sheets and stored at $21 \pm 2^\circ\text{C}$ for 65 days.

The rubber surfaces were inspected regularly and after a few days a white bloom appeared, which was examined in the SEM. There were needle-shaped objects covering the rubber surface entirely (Fig. 6). In some cases, bloom started from what appeared to be a centre on the rubber surface and radiated in all directions, producing a solid layer (Fig. 7) and sometimes, it formed a leaf-shaped pattern (Fig. 8).

FTIR analysis revealed characteristic bands for TBBS at 1641.48 cm^{-1} (Fig. 9a), antidegradant at 2362.88 cm^{-1} (Fig. 9b), and NR at 1126.47 cm^{-1} (Fig. 9c) in the spectrum to indicate their presence in the bloom (Fig. 9d). Notably, there were no bands for ZnO and silanized silica filler in the spectrum of the bloom (cf. Fig. 9e and Fig. 9f with Fig. 9d). For ZnO, a major band at 441 cm^{-1} using FT-Raman spectroscopy has been reported¹⁷ but FTIR could not detect this band. The presence of antidegradant in the bloom was expected, since it migrated to the surface to protect the rubber against environmental ageing.¹⁸ Small traces of NR in the bloom was from the rubber surface during the sampling of the solid layer before the FTIR spectrum was taken. TBBS and antidegradant were identified to be the main compounding ingredients that had undergone surface migration. As mentioned earlier, the

melting temperature of TBBS and antidegradant were below the curing temperature of the rubber, and both melted whilst the rubber was being cured at 140°C. When the cured rubber was removed from the mould and cooled down slowly to ambient temperature, TBBS and antidegradant diffused to the rubber surface forming the bloom. Clearly, there was excessive amount of TBBS in the rubber which did not react fully during the curing process.

Compound 2, which had 3 phr TBBS and 2.5 phr ZnO chemical curatives (Table I), was cured to produce thin sheets and then stored at $21\pm 2^\circ\text{C}$ for 65 days. The sheets were regularly inspected for bloom and there was no sign that the compounding ingredients had migrated to the rubber surface. However, when the rubber surfaces were analysed by X-ray, there were 17 %wt Zn and 7%wt O, as well as 48 %wt C, 3.4 %wt Si and 1.6 %wt S. In storage, ZnO continued blooming on the rubber surface covering over 80% of the surface area (Fig. 10).

Attenuated total reflectance (ATR) was used to chemically analyse the surface of this compound and there was no evidence of TBBS on the rubber surface (cf. Fig. 9a with Fig. 9g). However, a band at 2918.40 in the spectrum indicated presence of Santoflex 13 on the rubber surface (cf. Fig. 9b with Fig. 9g). Also a band at 2850.88 in the spectrum

signalled presence of the NR which was expected (cf. Fig. 9c with Fig. 9g).

Effect of the blooming of TBBS on the hardness of the rubber vulcanizate

The hardness of compound 1 increased by approximately 2.5% after 8 days and thereafter, it continued rising by an extra 2.7% after 65 days in storage (Fig. 11). This indicated that TBBS bloomed continuously in storage though at different rates. A similar trend was also observed for compound 2. However, for this compound, the hardness increased by 2.3% after 8 days and remained unchanged subsequently when the storage time was increased to 65 days. This suggested that ZnO stopped blooming after 8 days in storage.

Crack growth rate versus strain energy density of the rubber vulcanizates

Figure 12 and Figure 13 show dc/dn versus T on linear scales for compounds 1 and 2, respectively. There were two features evident on each figure. Firstly, for compound 1, dc/dn varied substantially linearly with T below 4 kJ/m^2 (Fig. 12) and for compound 2 below 3.5 kJ/m^2 (Fig. 13). Secondly, this linear relationship intersected the T axis at a finite value of about 0.44 kJ/m^2 for compound 1 (see insert in Fig. 12). This positive intercept was denoted by T_0 . Below T_0 , some crack growth occurred and this was solely attributed to

ozone and the rate of growth dc/dn was substantially independent of T . T_0 was interpreted as the minimum tearing energy at which mechanico-oxidative crack growth took place.¹⁹

Note that for compound 2, dc/dn continued rising as a function of T at the lower end of the results (see insert in Fig. 13) and no T_0 value was measured for this vulcanizate. For an unfilled sulfur-cured NR a T_0 of about 0.04 kJ/m^2 has been reported.¹⁹ It is also noteworthy that at the upper end of the results the deviation was attributed proximately to the catastrophic tearing energy T_c , at which crack growth rate approached infinity. Clearly, below T_c , dc/dn depended on T for both compounds.

Figure 14 shows dc/dn versus T results for compounds 1 and 2 on logarithmic scales. It was evident that the blooming of TBBS had a detrimental effect on dc/dn at a constant T . For example at about 0.28 kJ/m^2 , dc/dn increased by an order of magnitude as a result of the blooming of TBBS. The accumulative damage of the blooming of TBBS on dc/dn continued over the entire range of T and as T reached its highest level, i.e. 4.8 kJ/m^2 , dc/dn was almost 94% higher.

As mentioned earlier, values of the strain energy density, W , were calculated from

the area under the retraction curves after repeatedly cycling the test pieces until the force-extension curve settled to a virtually steady state after 7-10 cycles. The W values were used to calculate T , which was then plotted against the corresponding dc/dn to determine effect of stress relaxation and permanent set of the rubber during cycling on dc/dn . For instance, for compound 1 at 15% maximum strain amplitude, T was approximately 16% higher when effect of the permanent set on the rubber during cycling was not taken into account. This trend continued when the strain amplitude reached 40%. A similar feature was also observed for compound 2. Figure 15 shows dc/dn versus T on logarithmic scales for compounds 1 and 2. For both compounds, dc/dn increased because of higher T values. This was due to the dependence of dc/dn on T . Clearly, higher energies caused the crack to propagate faster in the rubber. However, this effect disappeared soon after a few cycles (cf. Fig. 4 with Fig. 5) and the energy reached a steady value at a constant maximum strain amplitude on the sample.

Examination of the internal structure of the rubber and fracture surfaces after cyclic fatigue tests

After the cyclic fatigue tests were completed, the fracture surfaces were examined in the SEM. There were two distinct regions on the fracture surfaces. Region near the rubber surface approximately 15-20 μm in size where there was a high concentration of re-agglomerated TBBS particles, labelled A in Fig. 16 and Fig. 17. These particles were up to 5 μm in size (Fig.18) and had a plate-like structure (Fig. 19). For compound 1, some of these particles were sticking out of the rubber surface (Fig. 20), creating an uneven surface (Fig. 21). This was due to the crystallisation of TBBS from supersaturated solution, which took place more readily near or on the surface than in the rubber itself.⁴ And region more towards the middle where the surface consisted of small scale localised tearing, which characterized slow incremental crack growth in the rubber under repeated stressing, labelled B in Fig. 16 and Fig. 17. Closer examination of region B at high magnifications showed the concentration of the re-agglomerated TBBS particles in compound 1 to be much higher than that in compound 2 (cf. Fig. 22 with Fig. 23).

Re-agglomeration of chemical additives caused tread cracking in tires. Re-agglomeration is defined to be physical re-arrangement of compounding ingredients after

vulcanization.² For example, in the groove of a natural rubber truck tire severe agglomeration was found throughout the tire. Repeated stressing of the rubber produced hairline cracks in most of the re-agglomeration areas, which illustrated their relative weakness under stress. Interestingly, longer stretching cycles on sections from the same tread produced tears that tended to follow a path through many agglomerated areas. The re-agglomerated areas were rich in zinc and sulfur. Treads with a high degree of non-carbon re-agglomeration had poorer resistance to crack development than those in which there were little or no re-agglomeration. The initiation of cracks and their subsequent growth under stress occurred more frequently in the regions of re-agglomeration. Furthermore, because these areas contained more sulfur and zinc oxide, they were over cured and this decreased their resistance to cracking². No data was produced to show effect of the agglomeration of the chemical curatives on dc/dn vs T of the vulcanizate. Re-agglomeration was reduced or eliminated by good dispersion of all the compounding ingredients. Notably, TBBS re-agglomerated more extensively in compound 1 because there was more of it in the rubber, i.e. 6 phr, and this caused resistance to crack growth to decrease. This subsequently resulted in a

higher rate of cut growth at a constant tearing energy. Rate of cyclic crack growth was also influenced by increases in the loading of carbon black²⁰. However, there has been little or no data available on the effect of the re-agglomeration of chemical curatives on the cyclic crack growth rate vs tearing energy for silica-filled NR vulcanizates.

Cure systems in industrial rubber articles for example tire treads consist of up to five different chemicals. They include primary and secondary accelerators, primary and secondary activators, and elemental sulfur, which may add up to 9.6 phr.²¹ Excessive use of the curing chemicals is harmful to health, safety, and the environment and their use is restricted by legislation. Precipitated silica pre-treated with TESPT is classified as a "crosslinking filler".²² Using 60 phr of this filler, the author and co-workers crosslinked and reinforced NR and substantially reduced the use of the curing chemicals in the rubber without compromising the good mechanical properties of the rubber vulcanizate.²³ To crosslink the rubber and optimize the chemical bonding between the rubber and filler via TESPT, 6 phr TBBS and 0.3 phr zinc oxide were added²² and as this work has shown TBBS bloomed to the rubber surface. However, when the ratio of TBBS to ZnO was changed to 3/2.5, the blooming of

TBBS stopped. This was an additional benefit of using a crosslinking filler such as silanized silica.

Conclusions

From this study, it was concluded that

1 – Tensile strips of natural rubber crosslinked and reinforced with 60 phr silanized silica

nanofiller containing a sharp edge crack were repeatedly stressed at a constant

maximum strain amplitude and test frequency and relaxed to zero strain in each cycle.

The crack grew and the rate of crack propagation was dependent on the level of the tearing energy.

2 – The rate of crack propagation increased significantly at a constant level of the tearing

energy when TBBS re-agglomerated in the rubber. The re-agglomeration had poor

resistance to crack development and this caused the rate of crack growth to increase by up

to 94% at a constant tearing energy. Therefore, the blooming of TBBS was largely

detrimental to the rate of cyclic fatigue crack growth in the rubber.

3 – TBBS re-agglomeration occurred more extensively near the rubber surface at a depth of

15-20 μm . When the TBBS/ZnO ratio was reduced from 6/0.3 to 3/2.5, the TBBS re-agglomeration decreased very significantly and this improved the resistance of the rubber to crack development and crack growth.

4 – Using 60 phr of a sulfur-bearing silanized silica nanofiller to reinforce and cure the rubber via the tetrasulfane groups of the silane by adding TBBS and ZnO at a ratio of 3/2.5 eliminated the blooming of TBBS. This was a more efficient use of these chemicals and as a result, it reduced damage to health, safety and the environment and produced a better quality rubber vulcanizate.

ACKNOWLEDGEMENT

The authors thank Evonik Industries AG of Germany for supplying the silica filler. The scanning electron microscopy of the samples was carried out at the Loughborough Materials Characterization Centre, UK. We are also grateful to DTR VMS Limited of UK (formerly Avon Automotive VMS) for supporting this project.

REFERENCES

1. Beatty, J. R. *Rubb Chem Technol* 1964, 37, 1341.

2. Hess, W. N.; Burgess, K. A. *Rubb Chem Technol* 1963, 36, 754.
3. Smith, R. W.; Black, A. L. *Rubb Chem Technol* 1964, 37, 338.
4. Van Amerongen, G. J. *Rubb Chem Technol* 1964, 37, 1065.
5. Lewis, J. E.; Deviney, M. L.; Wittington, L. E. *Rubber Chem Technol* 1969, 42, 892.
6. Ansarifar, A.; Critchlow, G. W.; Guo, R.; Ellis, R. J.; Haile-Meskel, Y.; Doyle, B. *Rubber Chem Technol* 2009, 82, 113.
7. Ansarifar, A.; Critchlow, G. W.; Guo, R.; Ellis, R. J.; Kirtley, S. P.; Seymour, B. *Rubber Chem Technol* 2007, 10, 148.
8. Saeed, F.; Ansarifar, A.; Ellis, R. J.; Haile-Meskel, Y.; Farid, A. S. *J Appl Polym Sci* 2011, In press.
9. Br Standards Institution. *Methods of Testing Raw Rubber and Vulcanized Compounded Rubber: Methods of Physical Testing, Part 3, Br Standard 1673*; Br Standards Institution: London, UK, 1969.
10. Br Standards Institution. *Methods of Test for Raw Rubber and Unvulcanized Compounded Rubber: Measurement of pre-vulcanizing and Curing Characteristics by*

Means of Curemeter, Part 10, Br Standard 1673; Br Standards Institution: London, UK;

1977.

11. Br Standards Institution. Methods of Test for Raw Rubber and Unvulcanized

Compounded Rubber: Measurement of pre-vulcanizing and Curing Characteristics by

Means of Curemeter, Part A60, Section 60.1, Br Standard 903; Br Standards Institution:

London, UK, 1996.

12. Wolff, S. Rubber Chem Technol 1996, 69, 325.

13. Br Standards Institution. Physical Testing of Rubber: Method for Determination of

Hardness. Br Standard 903: London, UK, 1995; Part A26.

14. International Organization for Standardization. Rubber, Vulcanized – Measurement of

Fatigue Crack Growth Rate. ISO 27727: Geneva, Switzerland, 2008.

15. Rivlin, R. S.; Thomas, A. G. J Polym Sci 1953, 10, 291.

16. Greensmith, H. W. J Appl Polym Sci 1963, 7, 993.

17. Jackson, K. D. O. Internet J Vibr Spect., [www.ijvs.com] 2, 3.

18. Jowett, F. Elastomerics 1979, 48.

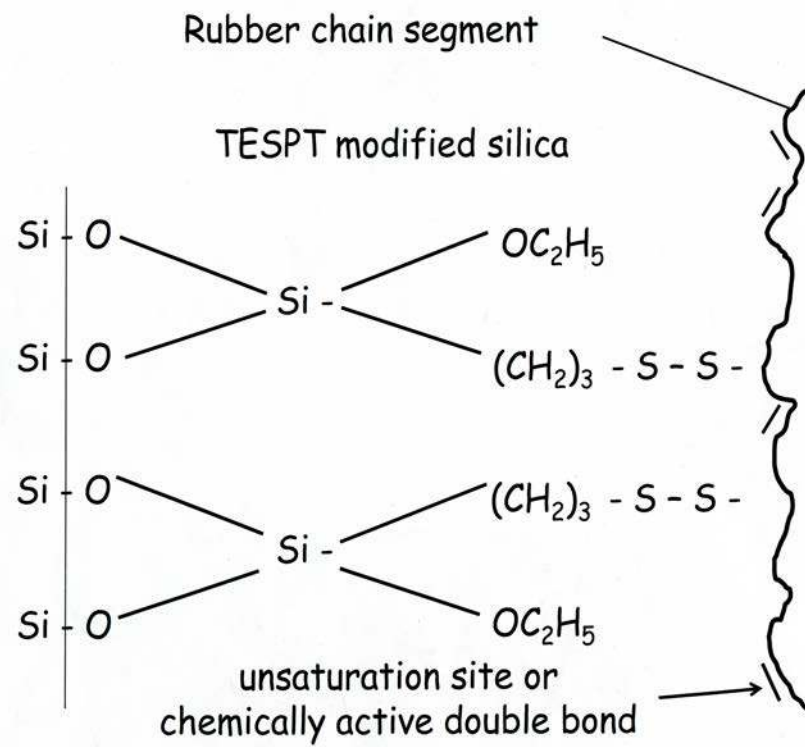
19. Lake, G. J. Paper presented at a meeting of the Rubber Division, American Chemical Society, Chicago, April 22, Paper A. 1994, Education Symposium: Fatigue in Rubber.
20. Auer, E. E.; Doak, K. W.; Schaffner, I. J. *Rubber Chem Technol* 1958, 31, 185.
21. Waddell, W. H.; Beauregard, P. A.; Evans, L. R. *Tire Technol Int* 1995, 14.
22. Rajeev, R. S.; De, S. K. *Rubber Chem Technol* 2002, 75, 475.
23. Ostad-Movahed, S.; Ansar Yasin, K.; Ansarifar, A.; Song, M.; Hameed, S. *J Appl Polym Sci* 2008, 109, 869.

TABLE I

Recipe, Mooney Viscosity and ODR Results for Compounds 1 and 2

Formulation (phr)	Compound	
	1	2
NR (SMRL)	100	100
Silanized silica	60	60
TBBS	6	3
ZnO	0.3	2.5
Santoflex 13	1	1
	Mooney viscosity (MU)	
	95	104
	ODR results at 140°C	
Minimum torque (dN m)	28	29
Maximum torque (dN m)	108	97
Δtorque (dN m)	80	68
Scorch time, t_{s2} (min)	9	10
Optimum cure time, t_{95} (min)	27	53
Cure rate index (min^{-1})	5.6	2.3

The compound temperature rose to 48-79°C during mixing.



Scheme 1. Silanized silica nanofiller pre-treated with TESPT. Tetrasulfane groups react with rubber to form stable covalent sulphur bonds.

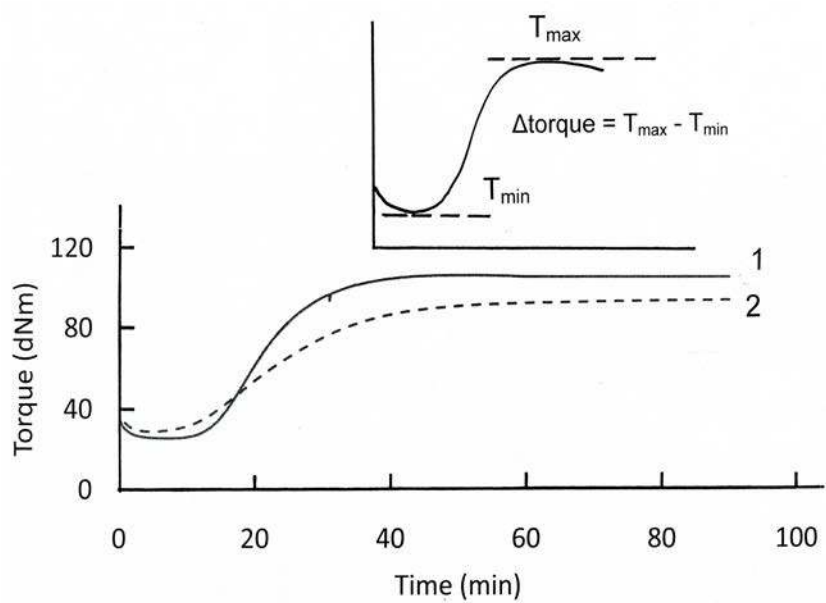


Figure 1. Torque versus time traces by ODR at 140°C for compound 1 and compound 2.

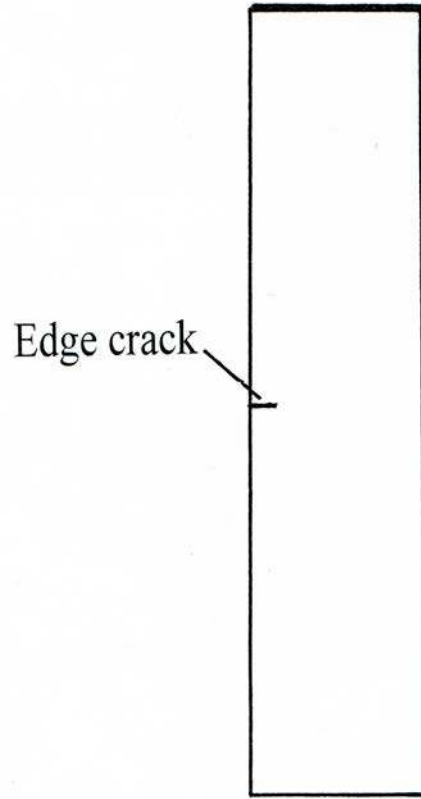


Figure 2. Tensile crack growth test piece with an edge crack.

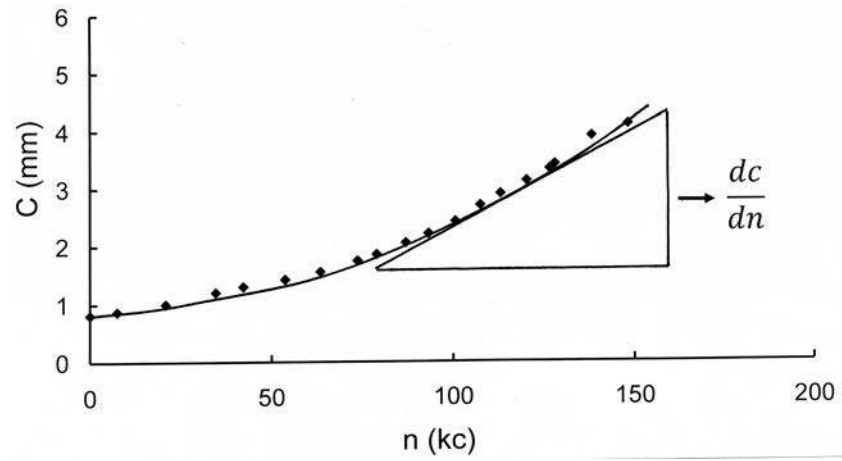


Figure 3. Crack length versus number of cycles from which dc/dn was calculated. Data for compound 1 at 40% strain amplitude.

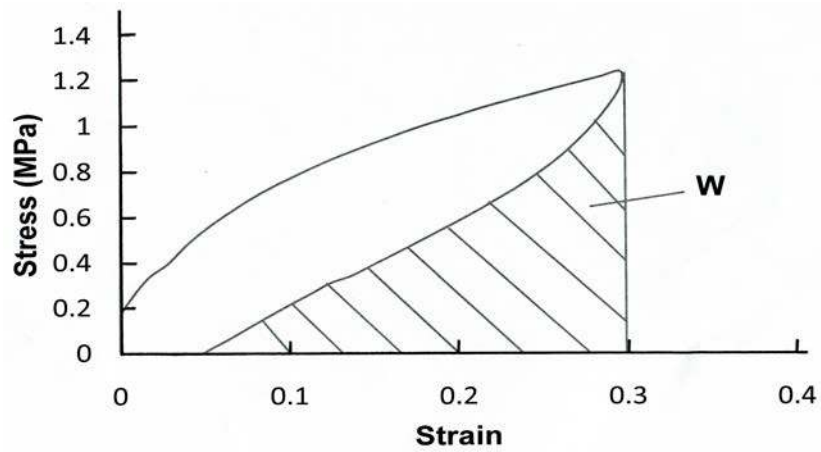


Figure 4. Stress versus strain data showing the area under the retraction curve where W was calculated from. Data for compound 2 after 1 cycle.

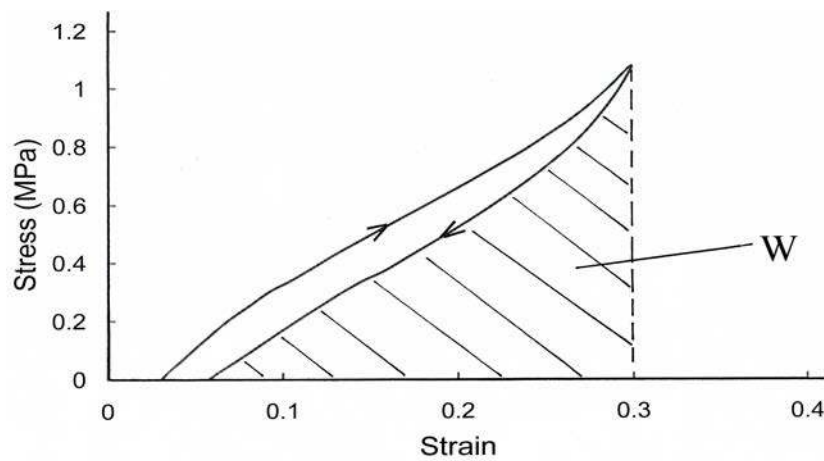


Figure 5. Stress versus strain data showing the area under the retraction curve where W was calculated from. Data for compound 2 after 10 cycles.

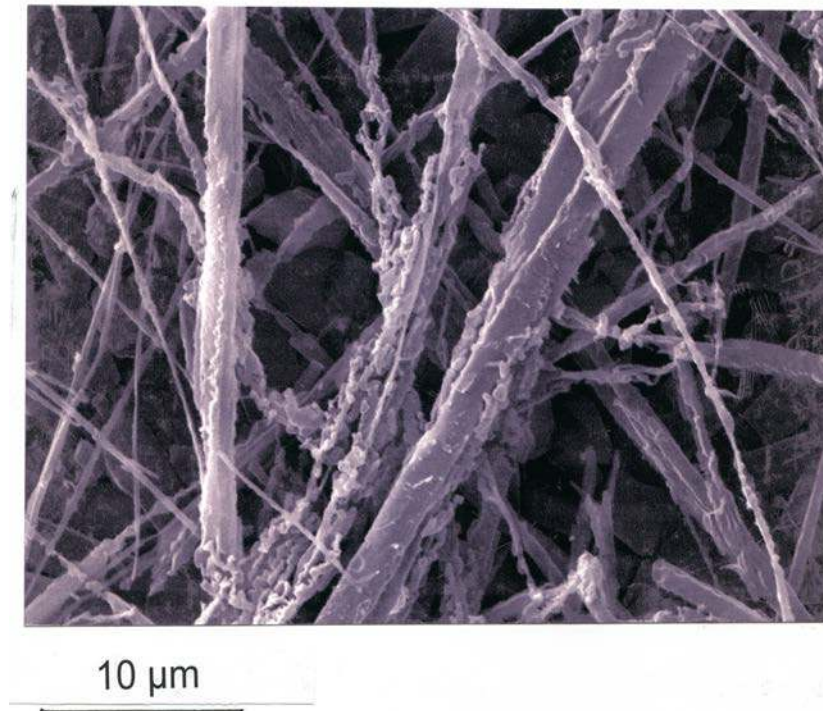


Figure 6. SEM micrograph showing needle-shaped objects on the surface of unstrained rubber. Storage time 65 days at ambient temperature. Data for compound 1.

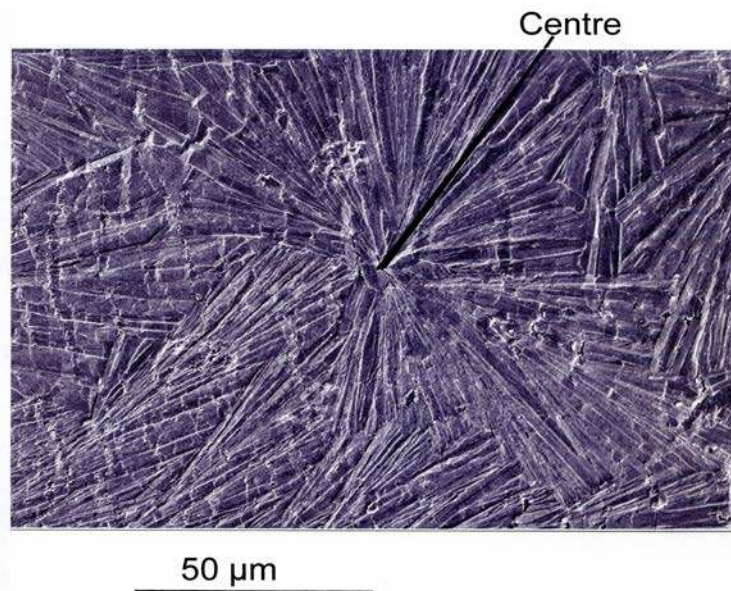


Figure 7. SEM micrograph showing bloom starting from what appears to be a centre on the surface of the unstrained rubber vulcanizate, radiating in all directions and producing a solid layer. Data for compound 1. Storage time 65 days at ambient temperature.

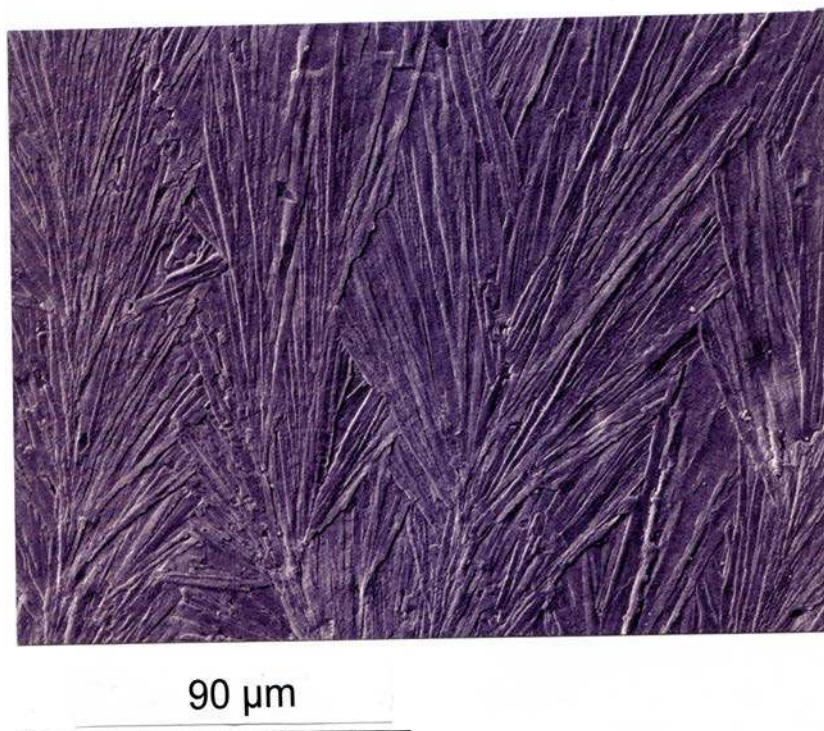


Figure 8. SEM micrograph showing a leaf-shaped pattern on the surface of the unstrained rubber vulcanizate. Storage time 65 days at ambient temperature. Data for compound 1.

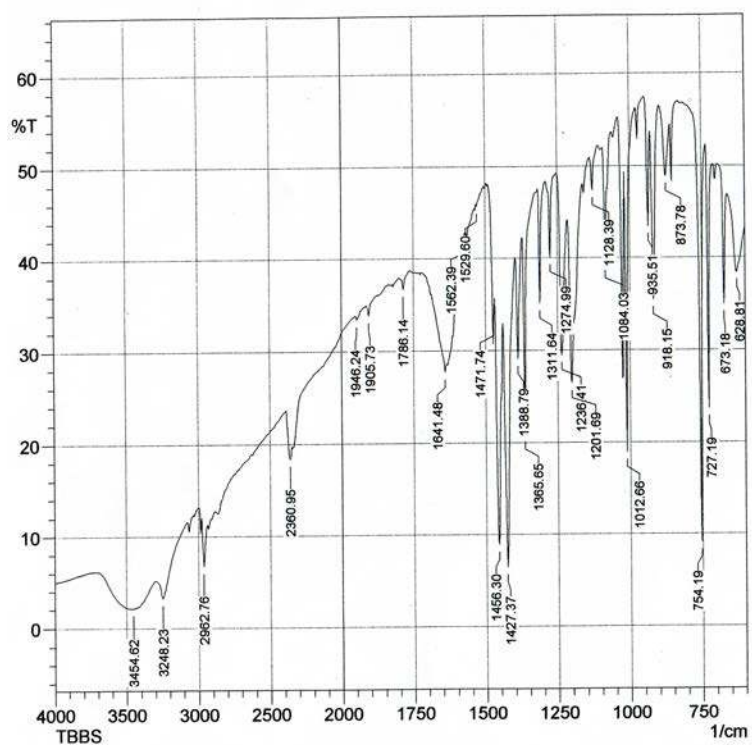


Figure 9(a) – FT-IR spectrum of TBBS. Horizontal axis is wavenumber.

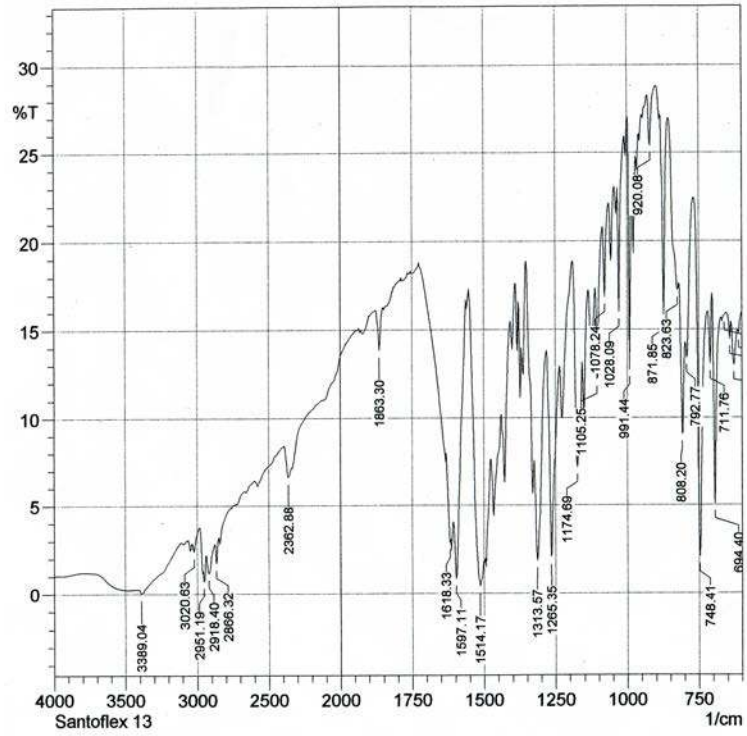


Figure 9(b). FT-IR spectrum of Santoflex 13. Horizontal axis is wave number.

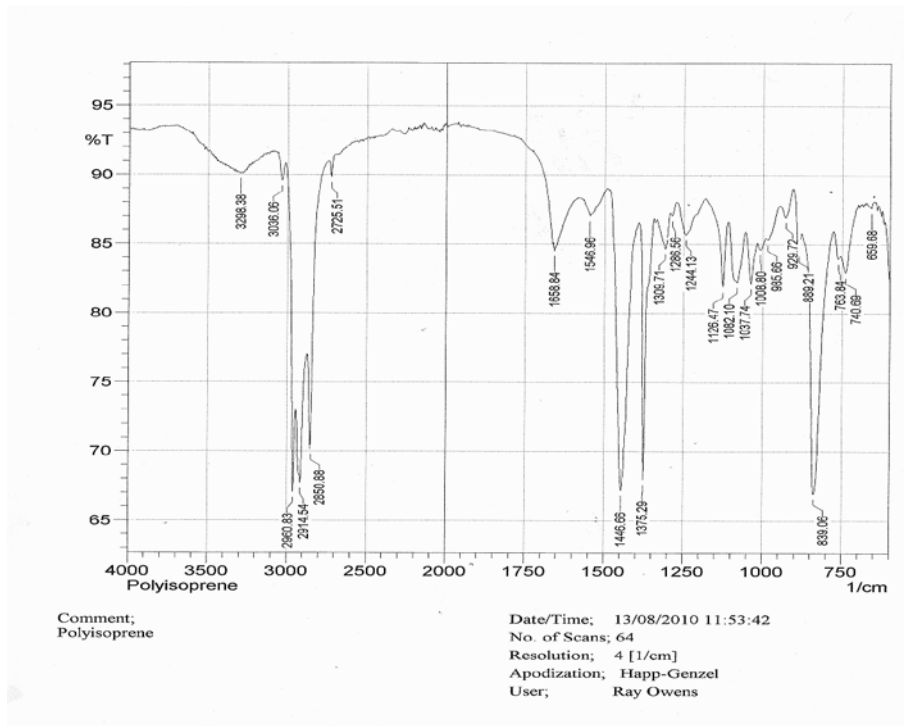


Figure 9(c). FT-IR spectrum of natural rubber. Horizontal axis is wave number.

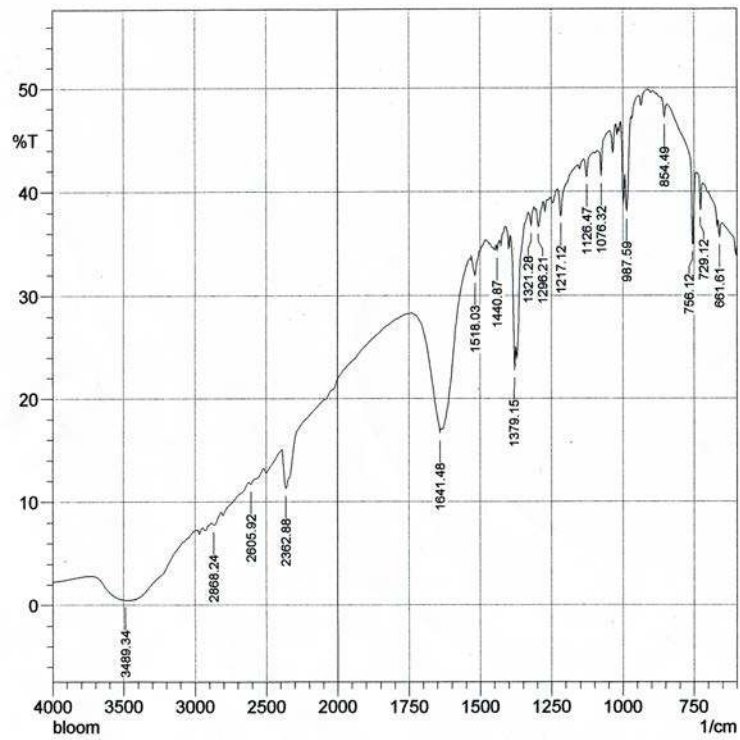


Figure 9(d). FT-IR spectrum of the bloom on the unstrained surface of cured compound 1. Horizontal axis is wave number.

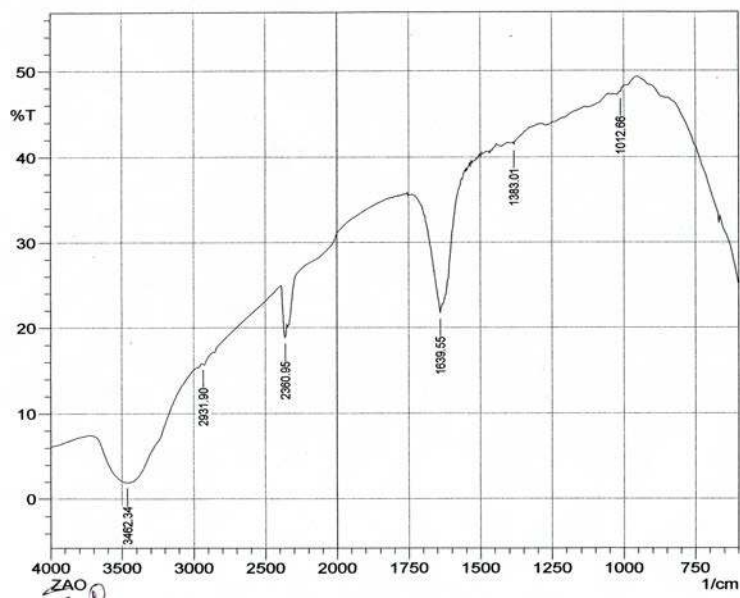


Figure 9 (e). FT-IR spectrum of ZnO. Horizontal axis is wavenumber.

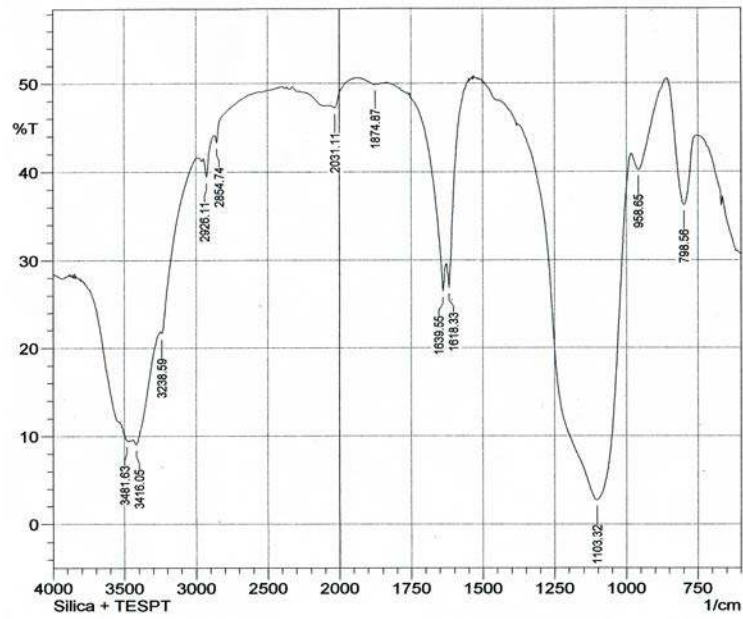


Figure 9(f). FT-IR spectrum of silanized silica nanofiller. Horizontal axis is wavenumber.

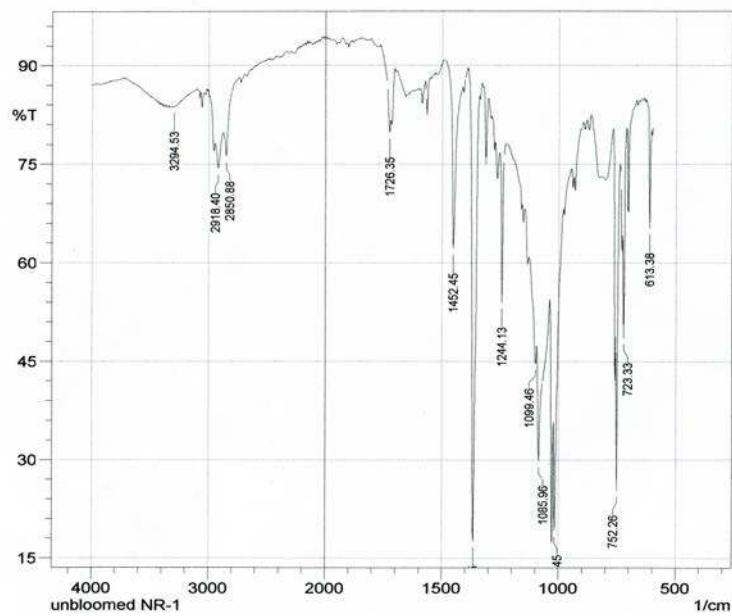


Figure 9(g). FT-IR spectrum from the unstrained surface of cured compound 2. Horizontal axis is wavenumber.

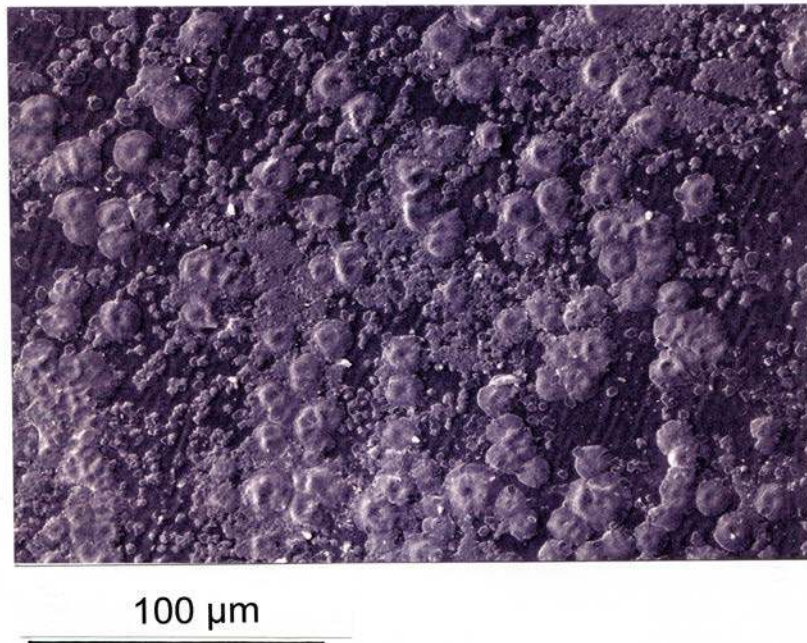


Figure 10. SDEM micrograph from the unstrained surface of compound 2 showing ZnO bloom. Storage time 8 days at ambient temperature.

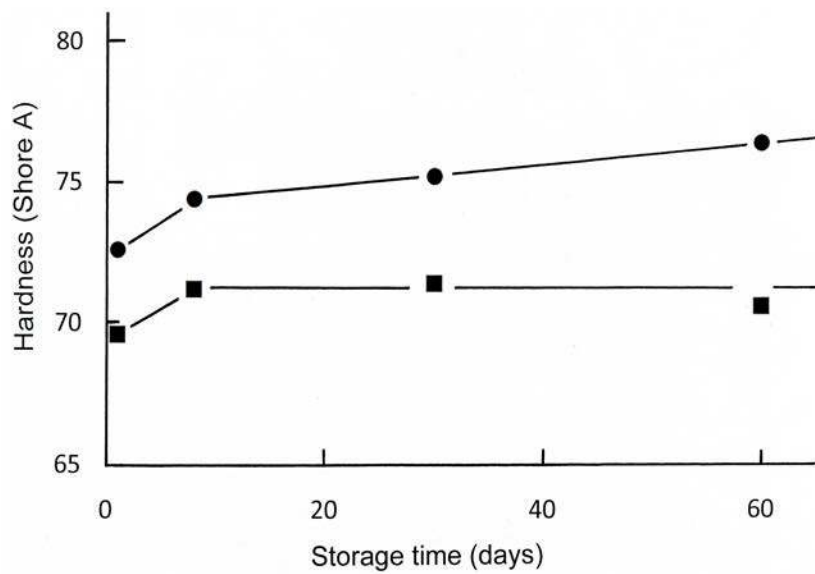


Figure 11. Hardness versus storage time. Compound 1 (●); Compound 2 (■).

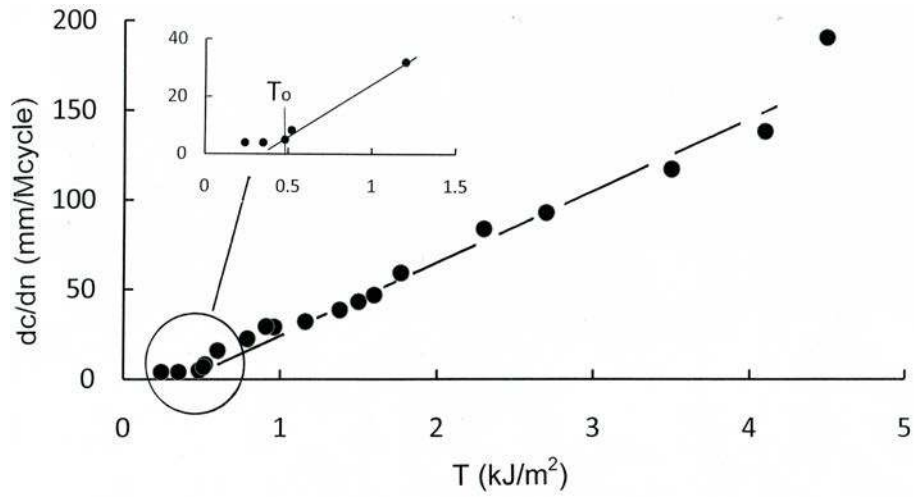


Figure 12. Crack growth rate dc/dn versus tearing energy T for compound 1. The insert shows the lower end of the results.

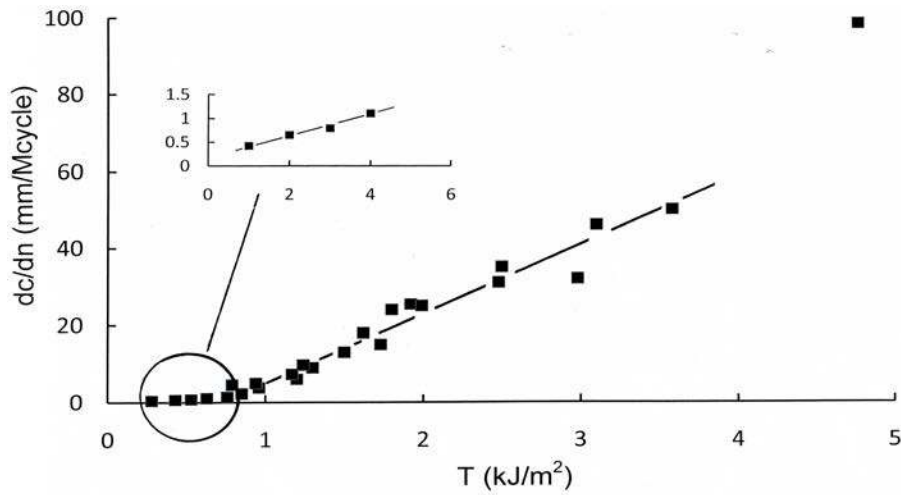


Figure 13. Crack growth rate dc/dn versus tearing energy T for compound 2. Insert shows the results at the lower end.

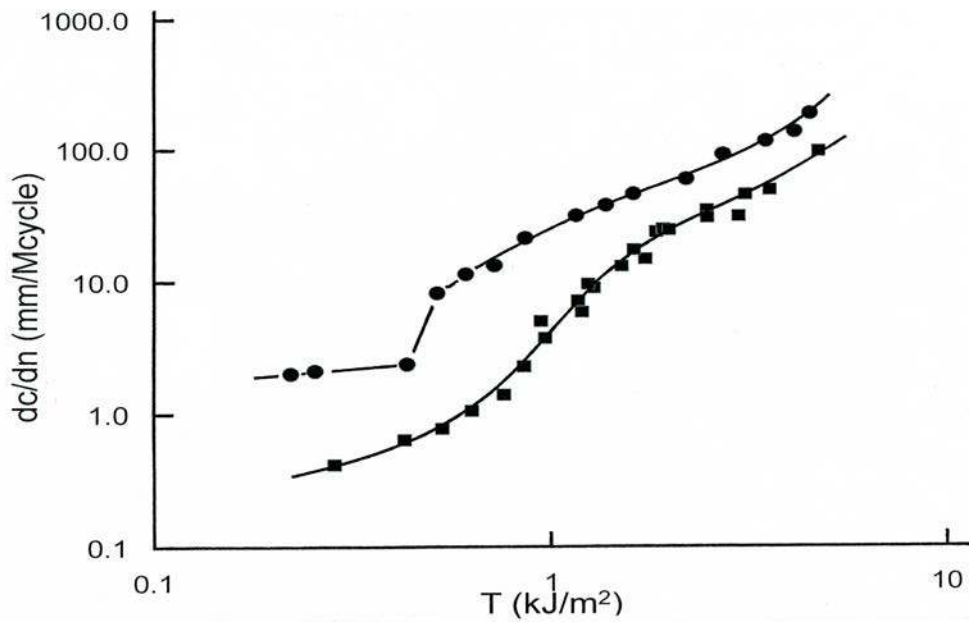


Figure 14. Crack growth rate dc/dn versus tearing energy T . Compound 1 (●), Compound 2 (■).

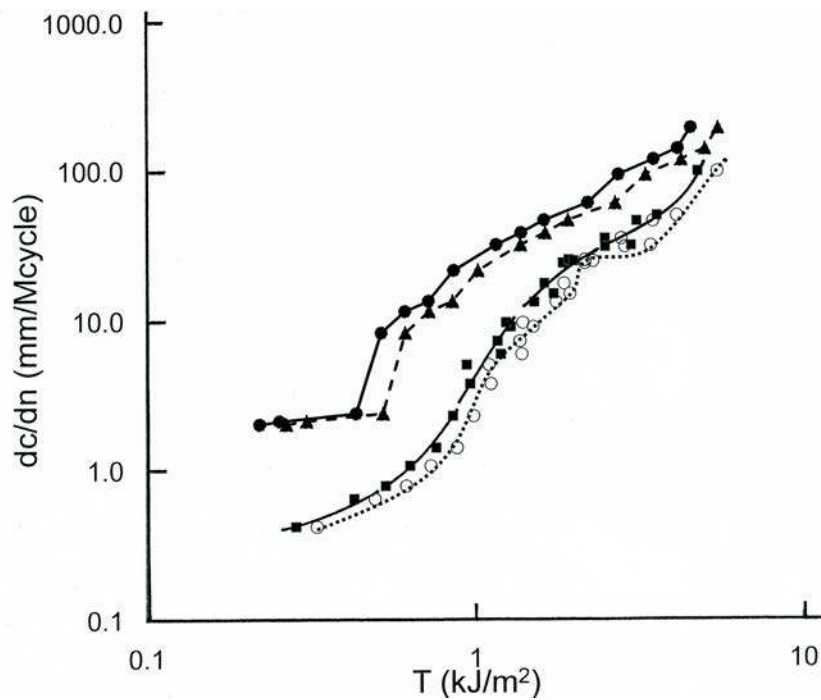


Figure 15. Crack growth rate dc/dn versus tearing energy T . Compound 1 with no allowance for stress relaxation in the rubber (●), with allowance for stress relaxation in the rubber (▲); Compound 2 with no allowance for stress relaxation in the rubber (■), with allowance for stress relaxation in the rubber (○).

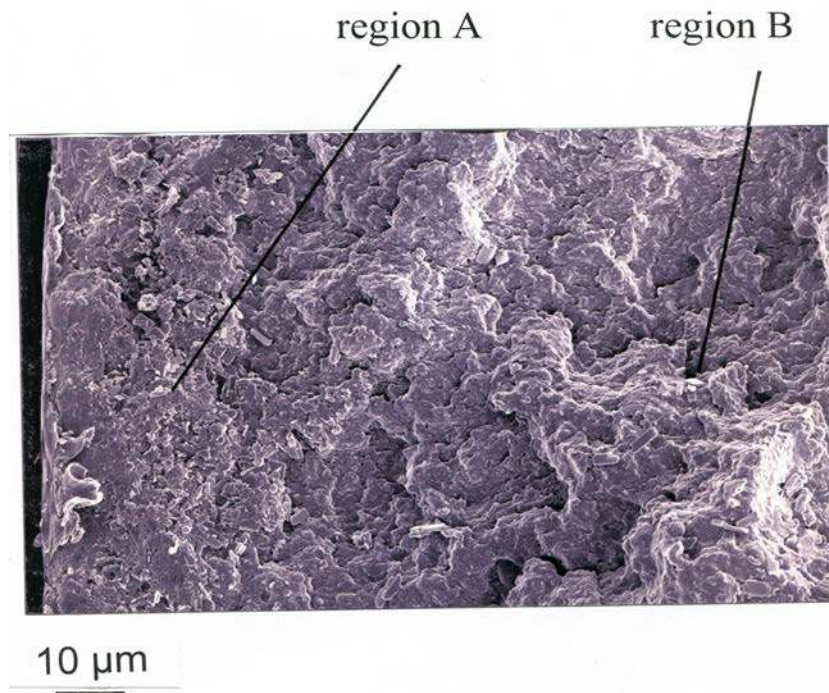


Figure 16. SEM micrograph from the fracture surface after fatigue test showing two distinct regions: region A and region B. Data for compound 1.

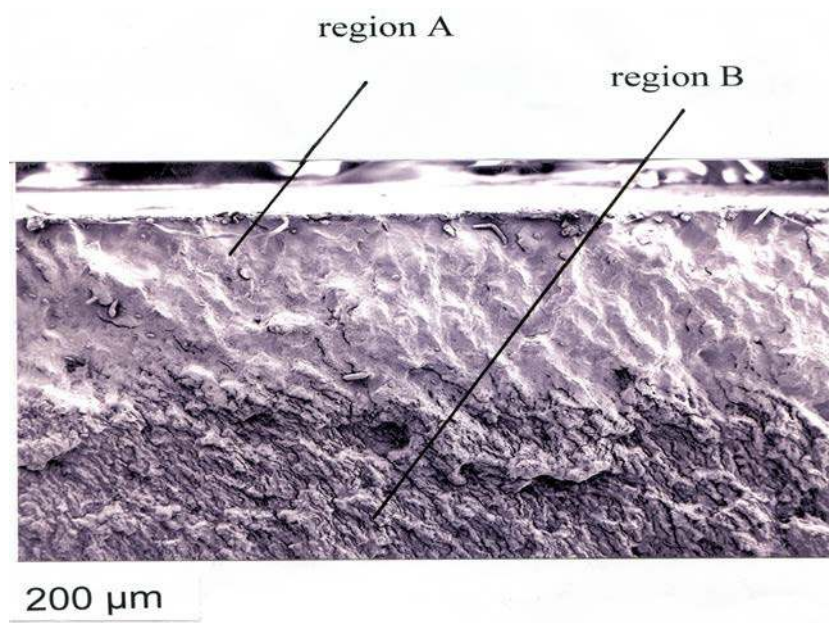


Figure 17. SEM micrograph from the fracture surface after fatigue test showing two distinct regions: region A and region B. Data for compound 2.

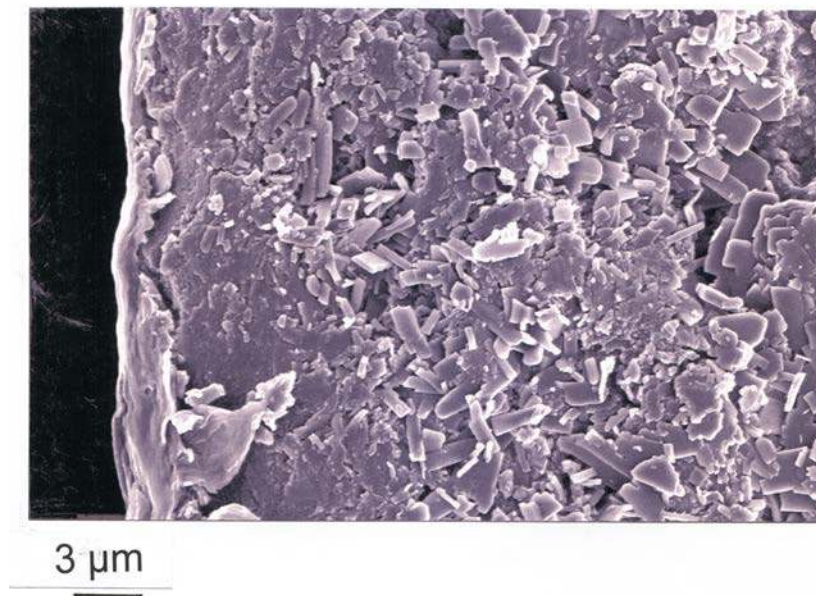


Figure 18. SEM micrograph after the fracture surface was recovered from fatigue test showing region A in Figure 16 at a high magnification. Data for compound 1.

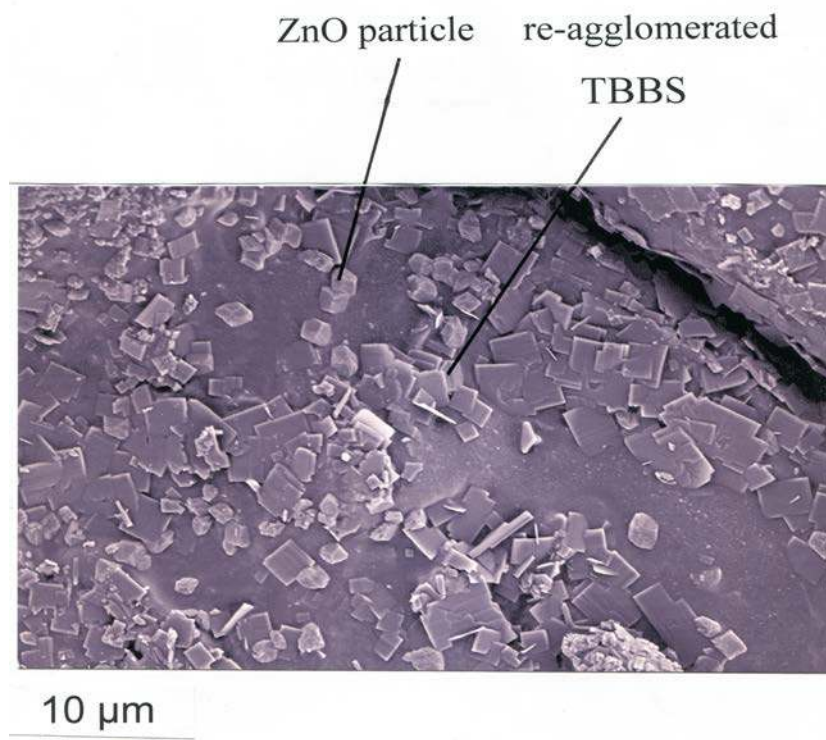
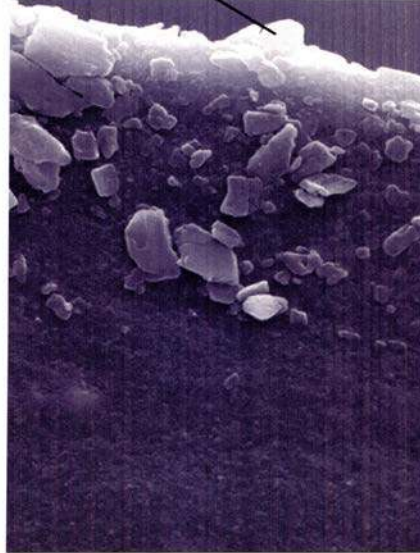


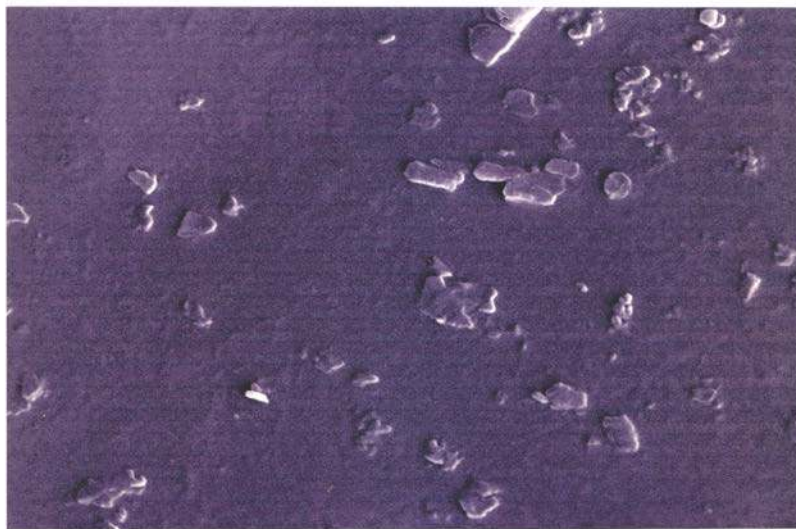
Figure 19. SEM micrograph after the fracture surface was recovered from fatigue test showing region A in Figure 17 at a high magnification. Data for compound 2.

re-agglomerated TBBS
sticking out of the
rubber surface.



10 μm

Figure 20. SEM micrograph after freeze-fracture test showing re-agglomerated TBBS particles sticking out of the rubber surface creating a rough surface. Data for compound 1.



10 μm

Figure 21. SEM micrograph from the unstrained rubber surface after bloom was removed by sellotape showing large solid particles in the rubber. Data for compound 1.

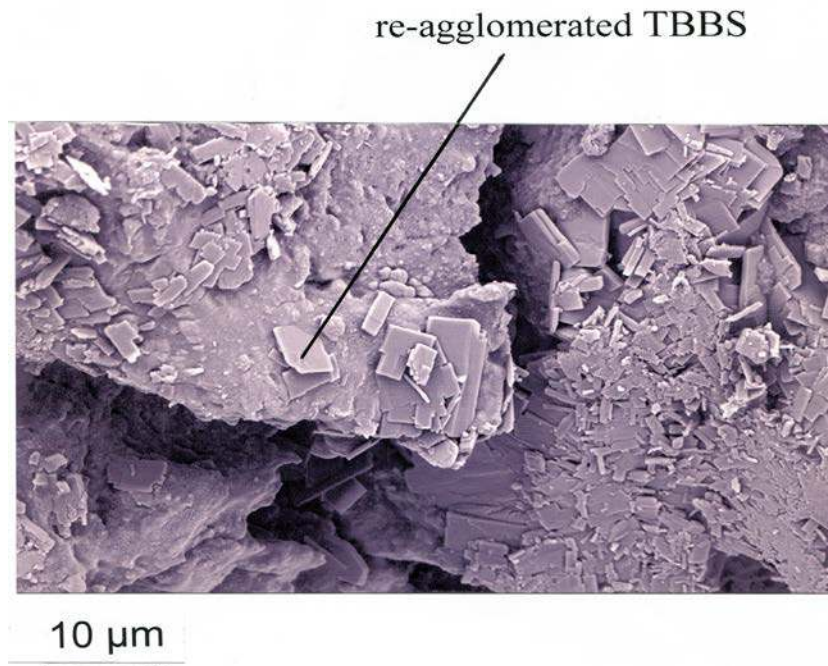


Figure 22. SEM micrograph showing re-agglomerated TBBS plate-like particles in the rubber in region B on Figure 16. Data for compound 1.

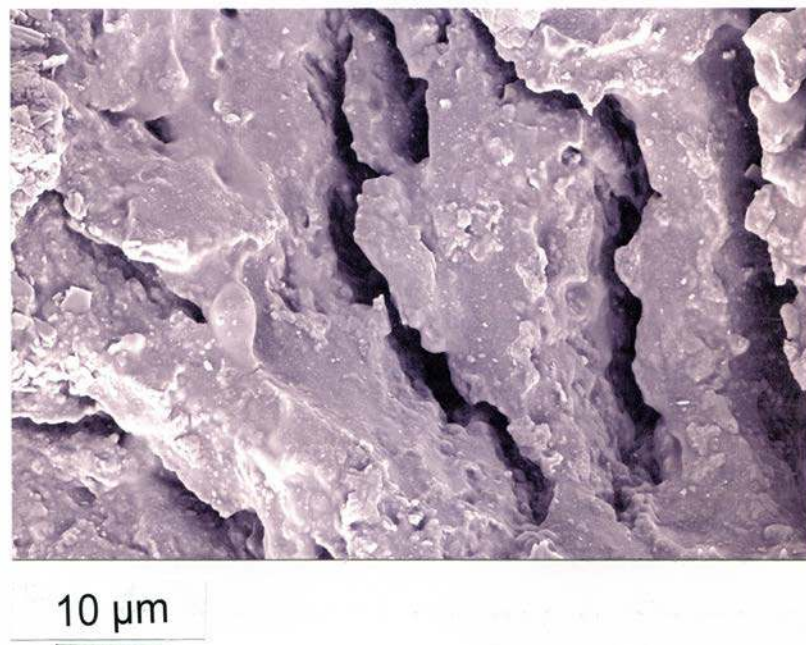


Figure 23. SEM micrograph after the fracture surface was recovered from the fatigue test showing region B on Figure 17 at a high magnification. Data for compound 2.